

Innovative shielding technique for wireless power transfer systems

Original

Innovative shielding technique for wireless power transfer systems / Canova, A.; Corti, F.; Laudani, A.; Lozito, G. M.; Quercio, M.. - In: IET POWER ELECTRONICS. - ISSN 1755-4535. - 17:8(2024), pp. 962-969. [10.1049/pel2.12580]

Availability:

This version is available at: 11583/2995415 since: 2024-12-16T09:25:34Z

Publisher:

John Wiley and Sons Inc

Published

DOI:10.1049/pel2.12580



Terms of use:

This article is made available under terms and conditions as specified in the corresponding bibliographic description in the repository

Publisher copyright

(Article begins on next page)

Innovative shielding technique for wireless power transfer systems

Aldo Canova¹ | Fabio Corti²  | Antonino Laudani³ | Gabriele Maria Lozito²  | Michele Quercio³

¹Politecnico di Torino, Dipartimento Energia (DENERG), Torino, Italy

²Università degli Studi di Firenze, Dipartimento di Ingegneria dell'Informazione (DINFO), Firenze, Italy

³Università degli Studi Roma Tre, Dipartimento di Ingegneria Industriale, Elettronica e Meccanica, Roma, Italy

Correspondence

Gabriele Maria Lozito, Università degli Studi di Firenze, Dipartimento di Ingegneria dell'Informazione (DINFO), Firenze, Italy.
Email: gabriele maria.lozito@unifi.it

Michele Quercio, Università degli Studi Roma Tre, Dipartimento di Ingegneria Industriale, Elettronica e Meccanica, Roma, Italy.
Email: michele.quercio@uniroma3.it

Abstract

The High Magnetic Passive Loop (HMCPL) technique is proposed as an innovative passive shielding system to mitigate the undesired dispersion of the magnetic field produced by a wireless power transfer (WPT) system, thus reducing the risk of hazardous human exposure. The magnetic structure is described both in terms of lumped parameters circuit, useful for sizing, and in terms of a geometrical representation solved by finite element method, useful to assess the field attenuation effects. Sizing of the resonance capacitors in the shielded WPT structure is approached as a Pareto optimization problem and solved via genetic algorithm. HMCPL shielding design guidance is provided to reduce the magnetic field emission in the surrounding environment. Furthermore, the influence of the shielding on the performance of the WPT system is also evaluated.

1 | INTRODUCTION

Wireless charging systems are increasingly common today for recharging electric vehicles (EV) [1–9]. One of the main issues for the development of the WPT is compliance with the electromagnetic fields (EMF) safety regulations [10–13]. Since the primary and the secondary coils are loosely coupled in air, a significant leakage magnetic field is dispersed in the surrounding area [14, 15]. Thus, some techniques to reduce the stray magnetic field that could interfere with nearby equipment or the human body are required. The systems that allow the mitigation of the magnetic field are divided into two macro-categories: active and passive shielding [16, 17]. In the first category, the shield is powered by external generators driven by a control system for tracking the field value and frequency. The second category can be further divided according to the type of material used for the shield, that is, ferromagnetic or conductive passive shielding. Passive ferromagnetic shielding exploits materials, such as iron, nickel, and cobalt, that have the ability to redirect or absorb magnetic fields. When a ferromagnetic material is placed in the path of a magnetic field, it creates an opposite magnetic field that partially cancels out the original field. Ferromagnetic shielding is effective against static and low-frequency magnetic fields. Conductive shielding involves the use

of materials with high electrical conductivity, such as copper or aluminum, to block or redirect magnetic fields. When a conductive material is placed in the path of a magnetic field, it induces eddy currents in the material. These eddy currents generate their own magnetic fields that oppose the original field, thereby reducing its strength.

In this work, an innovative HMCPL applied to an inductive charging system is presented. The proposed solution consists of a passive loop, made up of a circular coil, that is coupled to the WPT power transmission system by a ferrite core. This connection leads to a high coupling coefficient between the primary side and the shielding side producing in the screen conductor a current in an opposite phase with respect to the primary. The proposed solution has several advantages over the shielding techniques available in the literature. First, compared to active shielding, it does not need any control system for tracking the field value and the relative frequency [18]. As a result, the complexity of the system is greatly reduced. Since, through the coupling with the ferrite core, the supply frequency of the shield current is exactly that required, and the current, considering a unitary transformation ratio, is equal and opposite; consequently, the field generated by the shield will automatically have the opposite direction to the source. Compared to systems with ferrite and aluminum plate, this system is also

This is an open access article under the terms of the [Creative Commons Attribution License](https://creativecommons.org/licenses/by/4.0/), which permits use, distribution and reproduction in any medium, provided the original work is properly cited.

© 2023 The Authors. *IET Power Electronics* published by John Wiley & Sons Ltd on behalf of The Institution of Engineering and Technology.

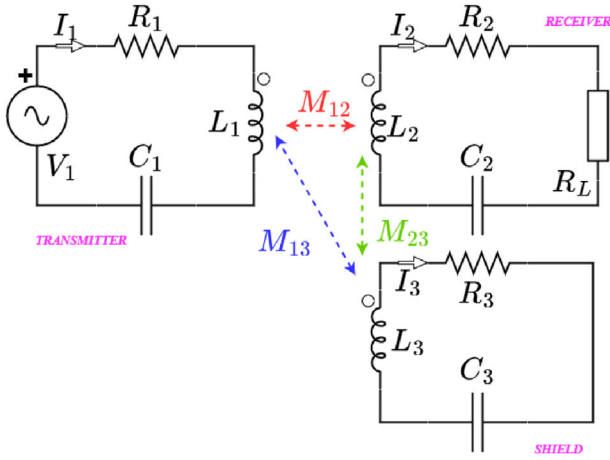


FIGURE 1 Equivalent circuit of the system with the three loops for transmitter, receiver and shield.

convenient from an economic point of view, as it requires a cable of the same size as that of the coil and a ferrite core specifically sized not to work in saturation condition. Furthermore, comparing the systems with aluminum and ferrite with the HMCPL, the advantage of the lower weight and overall dimensions is added. The novelty of the proposed paper lies in its introduction of a new technique to protect the magnetic field generated by a wireless power transfer (WPT) system designed for electric vehicle charging. The proposed solution belongs to the realm of passive screens. Differently from the shielding techniques available in the literatures, shields examined for similar purposes involved either ferrite components combined with an aluminum plate or active shielding systems that employed a powered coil to generate a magnetic field opposing the source magnetic field. The technique proposed is analyzed from different modelling point of views to create the design and performance assessment tools necessary for its practical implementation. Concerning the design, the WPT system with the presence of an auxiliary coil for shielding is represented in sinusoidal regime as a lumped parameters circuit [19–21]. The purpose of this circuit is to create a Pareto optimization problem to size the three resonance capacitors associated with transmitting, receiving and shield coils [22–24]. The problem aims at maximizing the current thorough the receiver and shield coils, while keeping their phase difference small to ensure the correct interference of the field generated by the shield. To define accurately the Pareto front, a powerful genetic algorithm suitable for such problems was used [25, 26]. After the system was properly sized, its performance was evaluated using FEM analyses through the use of COMSOL 6.0 Software. The performance evaluation was carried out by creating two inspection lines, one parallel to the other perpendicular to the WPT system on which the magnetic field and shielding factor (SF) values were evaluated. These evaluations were carried out both for the static and dynamic case. The results deriving from this study make it possible to identify HMCPL shielding as promising for this type of application, reaching in the static case near the shield an SF equal to 3 while in the dynamic case much higher SF values are reached. In this first work, the technique is presented

excluding the dimensioning of the ferrite core which creates the high magnetic coupling. The paper is organized as follows. First, the HMCPL is described, then, a 3D simulation with different configurations are provided to demonstrate the feasibility of the shielding system.

2 | MATERIALS AND METHODS

2.1 | Sizing of the resonant WPT system

In this section, the WPT system considering three coupled sections is studied in a sinusoidal regime to estimate the compensation capacitors. The equivalent circuit of the system considering the shield and the WPT transmitter and receiver is shown in Figure 1 along with the coupling elements.

The analysis of the circuit can be easily performed in sinusoidal steady-state through mesh analysis:

$$\begin{bmatrix} Z_1 & Z_{12} & Z_{13} \\ Z_{12} & Z_2 + R_L & Z_{23} \\ Z_{13} & Z_{23} & Z_3 \end{bmatrix} \begin{bmatrix} I_1 \\ I_2 \\ I_3 \end{bmatrix} = \begin{bmatrix} V_1 \\ 0 \\ 0 \end{bmatrix}, \quad (1)$$

where the impedances are shown below:

$$Z_p = R_p + j\omega L_p + \frac{1}{j\omega C_p}, \quad p \in \{1, 2, 3\}, \quad (2)$$

$$Z_{pq} = j\omega M_{pq}, \quad p \neq q; p, q \in \{1, 2, 3\}. \quad (3)$$

The capacitors are the quantities to be sized in this setup. An analytical expression for the resonance in the series-series configuration for a transmitter-receiver configuration is given by:

$$C_p = \frac{1}{4\pi^2 L_p f^2}. \quad (4)$$

This sizing equation can be used as a starting point for an optimization procedure that can refine the capacitor values. The optimization aims at the maximization of the load and shield currents imposing an efficiency above 90% (7), resulting in a two-dimensional Pareto problem, bounded considering a maximum angle between the shield and receiver current of $\pi/6$. Thus, the problem can be formalized as:

$$\max : |I_2(C_p)|, |I_3(C_p)|, C_p, p \in \{1, 2, 3\}, \quad (5)$$

$$\text{subj} : C_p > 0; \text{angle}\{I_2/I_3\} < \pi/6, \quad (6)$$

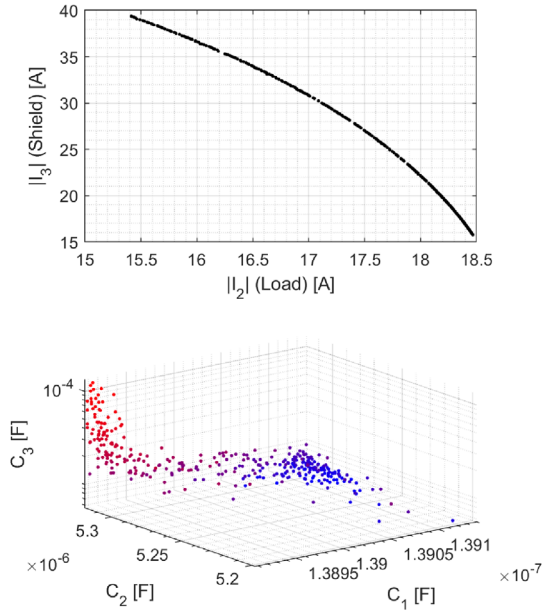
$$\eta = \frac{P_O}{P_I} = \frac{R_L \cdot |I_2|^2}{V_1 \cdot I_1 \cdot \cos(\phi_1)} > 90\%, \quad (7)$$

where:

- P_O : Power output
- P_I : Power input
- ϕ_1 : phase shift between the primary voltage V_1 and the primary current I_1

TABLE 1 Equivalent circuit parameters.

L_1 [μH]	L_2 [μH]	L_3 [μH]	M_{12} [μH]	M_{23} [μH]	M_{31} [μH]
28.2	20.7	0.832	7.71	0.308	0.116
R_1 [$m\Omega$]	R_2 [$m\Omega$]	R_3 [$m\Omega$]	R_L [Ω]	f [kHz]	V_1 [V]
100	100	100	10	85	20

**FIGURE 2** Pareto Optimization for the determination of the three capacitance. Optimized current values are shown on top. Capacitance values in the solution space are shown on the bottom: red points favor current on the load, blue points favor current on the shield.

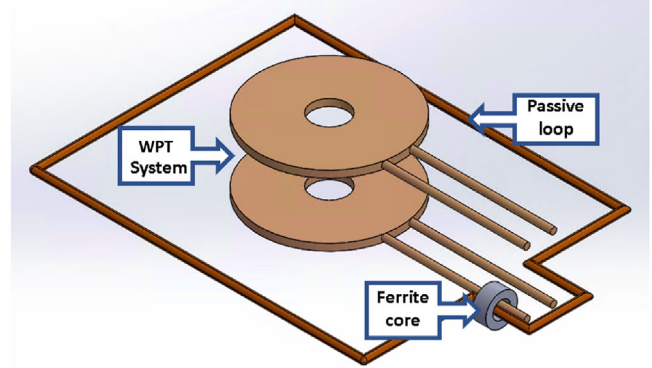
Considering the circuit parameters shown in Table 1 referring to the optimized geometry:

The resulting optimization leads to a Pareto front shown in Figure 2.

The optimization is performed in Matlab R2022b environment through the NSGA-II (non-sorting genetic algorithm), which is a multi-objective evolutionary algorithm based on a non-dominated sorting approach. The algorithm is widely used for these kinds of problems in literature due to convergence performance and the inherent capability of spreading the solutions over the Pareto front, thus ensuring the possibility of visually investigating the trend of the solutions in the solution space. The algorithm is implemented as a standard function in MATLAB R2022b environment. Due to the simple nature of the optimization problem, the algorithm did not require a further local optimization strategy, nor a specific initialization to avoid local minimum entrapment. The population size was set at 1000 individuals and a stopping criterion at 3000 generations was set but not reached. All other options were left as defaults. The optimization was both lower and upper bounded around the guess value C_p given by (4). A factor of 0.1 was used for lower bound and a factor of 10 was used for the upper bound. The machine used for the optimization is a Core i7 10th Gen with 16Gb of

TABLE 2 Three solutions to the Pareto optimization problem.

Type	C_1 [nF]	C_2 [μF]	C_3 [μF]
Pr.Load	138.2	5.311	108.2
Pr.Shield	139.8	5.291	5.633
Balanced	139.1	5.299	10.02

**FIGURE 3** Simplified geometrical representation of the HMCPL shielding technique applied to wireless power transfer system.

RAM. Pareto front was defined after about 900 generations of the genetic algorithm, which were computed in less than 2 min.

From the optimization, three numerical solutions are identified on the Pareto front: the first prioritizes load current over shield current, the second prioritizes shield current overload current, and the third gives equal importance to both currents (achieving, obviously, lower currents for both shield and load). Results are reported in Table 2.

2.2 | HMCPL theoretical analysis

The HMCPL allows the mitigation of the field produced by the WPT system through the use of conductors wound in loops strongly coupled to the source (transmitter coil) (Figure 3).

The operating principle is based on Faraday's law; the alternating magnetic flux generated by the transmitting coil creates an induced current in the shield circuit so that the magnetic field produced by the latter compensates for the source field (Lenz Law). The shield is constituted by a short-circuited coil with a very low series resistance. Due to magnetic coupling with the transmitter coil via ferrite core, the current flowing through it is a portion of the supply current of the WPT system, given by a transformation ratio. Said t the transformation ratio, it is described as:

$$t = \frac{N_2}{N_1}, \quad (8)$$

where:

- N_1 : Number of turns of the primary (source)
- N_2 : Number of turns of the secondary (shield)

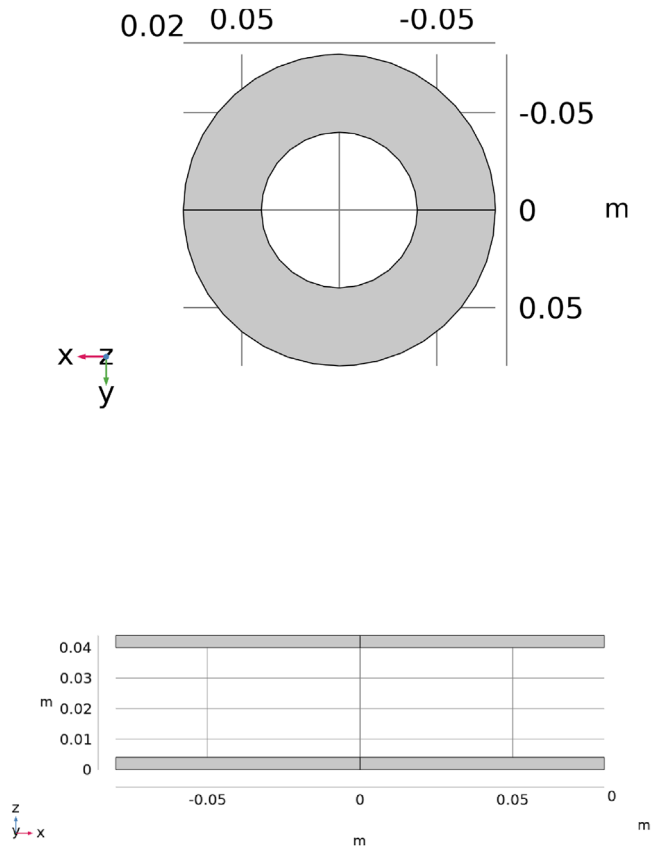


FIGURE 4 WPT geometry simulation.

Consequently, the induced current in the shield (I_{shield}) can be estimated as:

$$I_{shield} = \frac{I_{source}}{t} \quad (9)$$

The material used for the core was a N82 ferrite core. The choice was made by appropriately sizing the core to work in a non-saturation condition.

2.3 | HMCPL: 3D-simulation

To assess the shielding performances of this methodology and its effects in terms of WPT performance, a geometrical 3D simulation of the full system must be performed. For this purpose, the system was implemented as a 3D model in COMSOL 6.0. The feasibility and validation of this shielding method were first simulated on the system of circular coils shown in Figure 4 whose characteristics are listed in Table 3.

Given the geometry, a simulation relating to the magnetic field produced by the transmitting coil without the presence of the shield was conducted. This simulation acts as a baseline necessary for the evaluation of the shielding effectiveness parameter. For this purpose, the voltage was chosen as the coil excitation parameter, set at a value of 12 V for the transmitter. The chosen working frequency is 85 kHz. The evaluation of

TABLE 3 WPT system characteristics.

	$Coil_{transmitter}$	$Coil_{receiver}$
D_e [cm]	17	17
D_i [cm]	8.5	8.5
s [mm]	4	4
N_{turns}	14	12

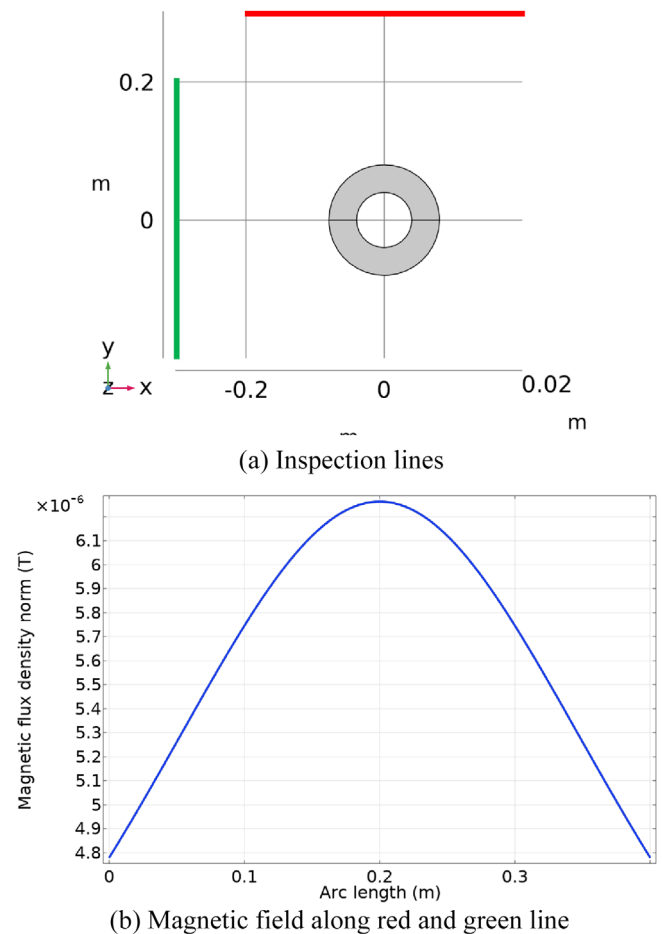


FIGURE 5 Magnetic field along inspection lines without the shield.

the magnetic field values was carried out by choosing a parallel inspection line (red) and a perpendicular inspection line (green) on the same plane as the transmitting coil, 30 cm away and 40 cm long (Figure 5a). Figure 5b shows the magnetic field values in the vicinity of the WPT system in the absence of a shield. It reaches a maximum value of $\approx 6.2\mu T$. So, to mitigate these values a loop was introduced as a screen (Figure 6). The chosen geometry is the circular one like the transmitting coil and the dimensions have been evaluated through an exhaustive search, which has shown that the problem has a single global minimum and thus a single optimal radius of the circle can be determined. The dimension deriving from this investigation is $R_{shield} = 10$ cm, $s_{shield} = 4$ mm equal to litz conductor diameter (Figure 6). To avoid a larger thickness, a single winding is used for the shield

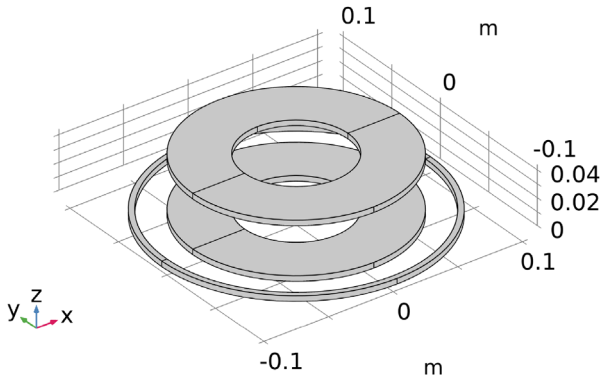


FIGURE 6 HMCPL applied to WPT system.

coil, thus $N_3 = 1$. Looking now at Equation (9), the calculation of the current value to be imposed on the shield conductor is necessary and important in order to establish the number of primary and secondary windings on the ferrite core of the HMCPL system. At this point, the choice of the current value to be imposed on the shield depends on the desired shielding factor (SF) defined as:

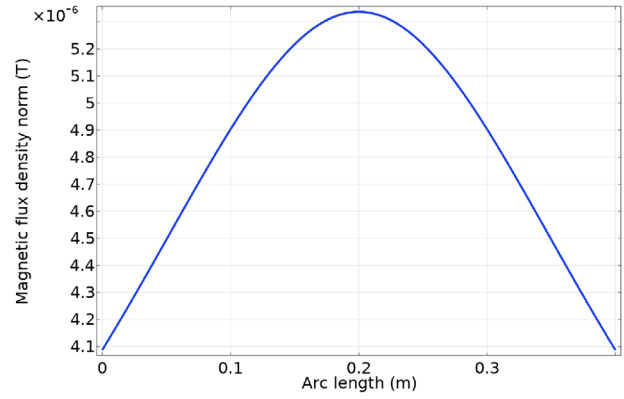
$$SF = \frac{|B_0(x, y, z)|}{|B_S(x, y, z)|}, \quad (10)$$

where:

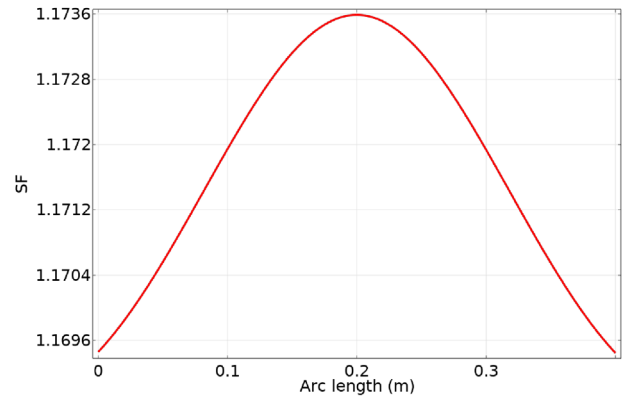
- B_0 is the magnetic induction at a certain point when the shield is absent.
- B_S is the equivalent with the screen applied.

Considering the transformation ratio t equal to one for simplicity, the value of the current imposed on the shield is equal but opposed in sign to that of the transmitter. So, the SF of such screen is shown in Figure 7b. However, this solution affects the coupling between the transmitter and receiver coils. This has been evaluated by calculating the power P_O on a resistance of 10Ω connected to the receiving coil and acting as a load (as already considered in the lumped parameters circuit optimization described before) with and without the presence of the shield. The active power dissipated by the resistive load without the presence of the shield is $P_{load} = 30 \text{ W}$. With the introduction of the shield, the power drops to $P_{load}^{sh} = 18 \text{ W}$, as shown in Table 4.

The drop in delivered power highlight that the effect of the shield weakens the magnetic field distribution in the geometry as desired. However, this process hinders the power transfer to the load, which is not acceptable in a WPT system. For this purpose, a modified geometry is proposed for the shield with the purpose of containing the reduction of the transferred power while retaining the shielding capabilities in the vicinity of the WPT system.



(a) Magnetic field along red and green line



(b) Shielding factor trend

FIGURE 7 Effect of the HMCPL shield along inspection lines.

TABLE 4 Power on the load of the receiver coil.

	$P_{load} [\text{W}]$	Efficiency [%]
No-shielding system	30	98.3
With shielding	18	97.6
With optimized shielding	30	98.1

2.4 | Alternative geometry and geometrical parameters optimization

The shielding system should be able to retain the effects in the vicinity of the WPT system to reduce exposure to harmful magnetic fields, while reducing its shielding effectiveness in the area closer to the WPT coils, to contain the power drop phenomenon. To achieve this result, an alternative geometry based on a double conductor proposed and optimized. The geometry is shown in Figure 8.

The parameters that characterize this new geometry are the radius of the inner circumference R_{shield_i} , the S and W parameters as shown in Figure 8. In order to determine the optimal parameters, several simulations were conducted to analyze the influence that each of them have on the magnetic field values evaluated along the previously defined inspection lines. The value R_{shield_i} was evaluated in the previous case and kept constant in this analysis, while the other two parameters S and W were made to vary.

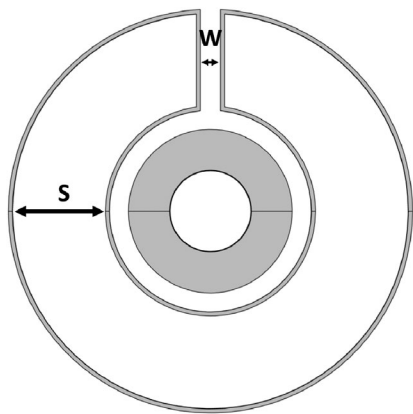
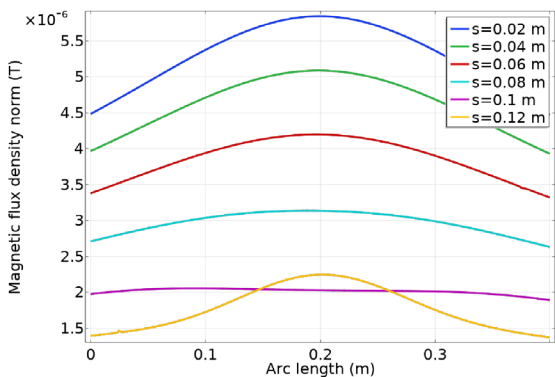
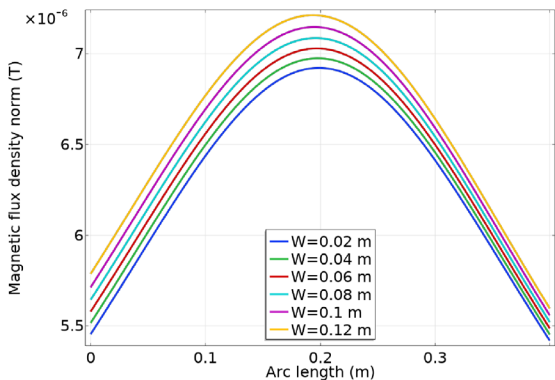


FIGURE 8 HMCPL optimized geometry.



(a) Effect of S parameter on magnetic field



(b) Effect of W parameter on magnetic field

FIGURE 9 Effect of the new shield shape along inspection lines.

The results are shown in Figure 9 where only the values taken along the red inspection line are represented, which is considered more critical in this case as it faces an area where it is not closed or where the W parameter is represented.

From the results of the previous simulations, it can be seen that the optimal parameters for a decrease in the magnetic field along the inspection lines are, respectively, $S=0.1$ m, $W=0.02$ m. Consequently, by imposing these values and carrying out a new simulation, the magnetic field and shielding factor values along the inspection sections were evaluated. The data are reported, respectively, in Figures 10–13. What can be seen from

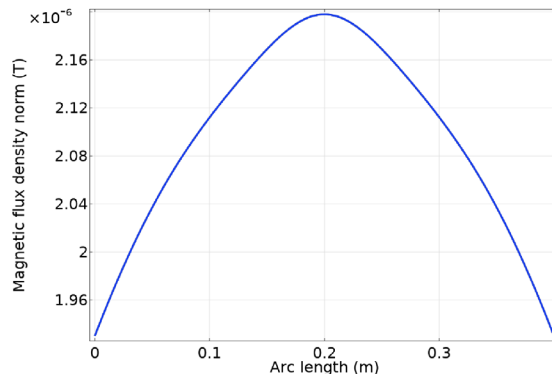


FIGURE 10 Magnetic field along red line.

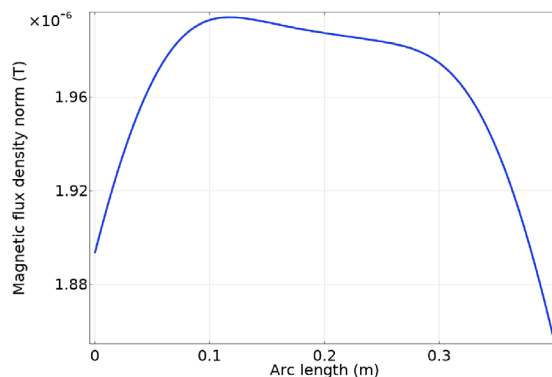


FIGURE 11 Magnetic field along green line.

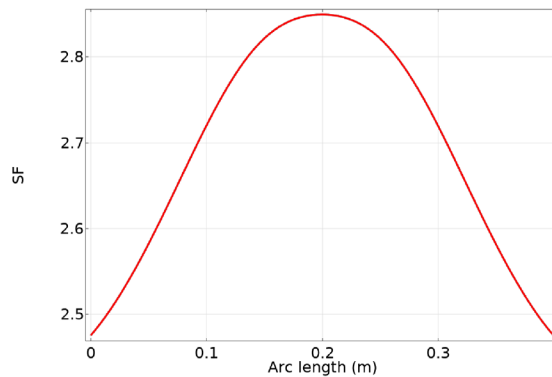


FIGURE 12 SF along red line.

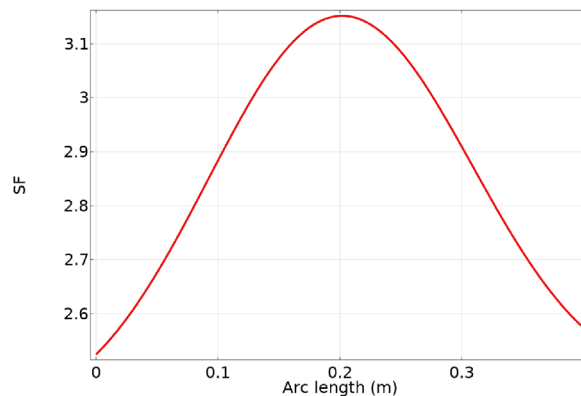


FIGURE 13 SF along green line.

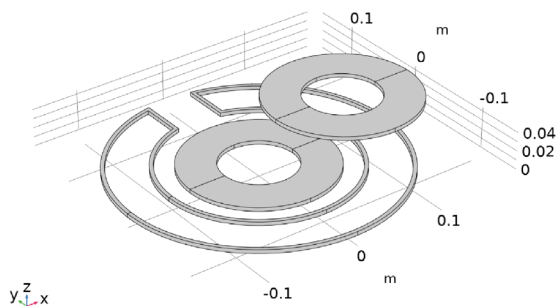


FIGURE 14 WPT misalignment case 0.1 m.

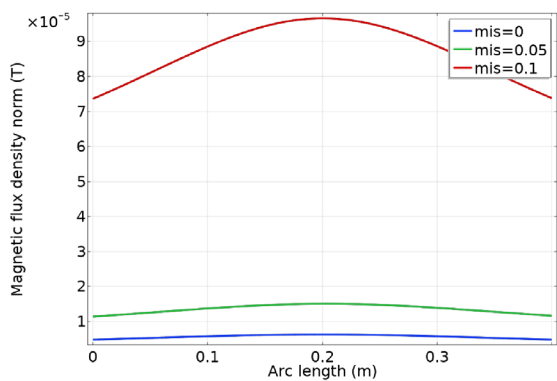


FIGURE 15 Magnetic field along inspection line in misalignment case without shield.

the reported data is that the power transmission system is not influenced by the presence of the shield and compared to the case of the circular shield, the shielding factor is improved. The next step was to evaluate this shielding system in the worst case of the WPT or that of the misalignment between the transmitting and receiving coil.

2.5 | Misalignment

Misalignment is a condition of particular interest for this study due to its effect both in terms of transmitted power, and in terms of effects of the shielding system. The geometrical effect is seen in Figure 14, which shows the WPT system in the misaligned case. Three different configurations were evaluated as a function of the distance of the misalignment. From a dosimetric point of view, these cases are considered the worst as there is a poor coupling between the two coils and therefore there are many fluxes of magnetic field dispersed in the air (Figure 15). Also for these cases, the effect of the screen is positive as shown in Figures 16 and 17. Even in the most distant case between the coils, there is a significant shielding factor. It should be considered that the values shown refer to the red inspection line, that is, the one facing parameter W , as between the two lines it is considered the worst case, especially in this case where the coil transmitter moves away from the green inspection line.

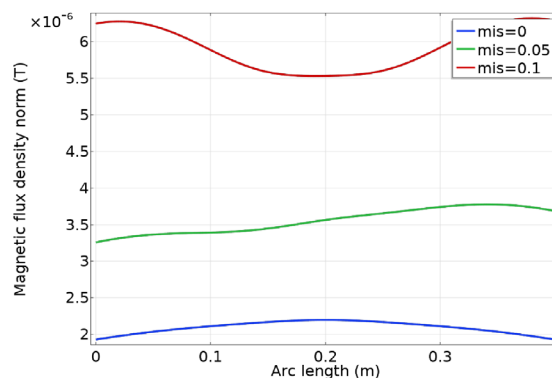


FIGURE 16 Magnetic field along inspection line in misalignment case with shield.

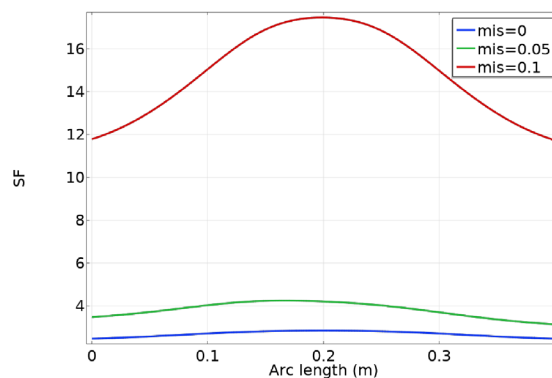


FIGURE 17 SF misalignment case red inspection line.

3 | CONCLUSION

The HMCPL system used to screen three-phase distribution lines was implemented for the first time in a WPT system. The advantages of this passive shielding system are many, among these, it is worth mentioning the fact that compared to active shielding, the complexity of the system is reduced and the shielding results as shown in the work are remarkable. Therefore, from the simulations and experiments conducted, it can be stated that this technique is effective in shielding the magnetic field produced by this power transmission system, without altering its effectiveness. This work places the necessary foundation for experimental validation of this shielding technique, since it formalizes a model both at geometrical and at lumped parameters level. Several critical aspects should be considered in the creation of the experimental validation workbench. First, a controlled environment is needed to ensure that the shielding effectiveness is evaluated correctly. Second, the non-linearity introduced by the ferrite coupling could introduce unwanted harmonics [27–31]. Third, the power source could exhibit a current dependant efficiency which could reduce the overall transmitted power as a function of the load current. Thermal analysis will also be carried out to investigate the influence of temperature on the performance of the WPT system and the screen.

AUTHOR CONTRIBUTIONS

Aldo Canova: Writing — review and editing. **Fabio Corti:** Writing — review and editing. **Antonino Laudani:** Writing — review and editing. **Gabriele Lozito:** Writing — review and editing. **Michele Quercio:** Writing — review and editing.

CONFLICT OF INTEREST STATEMENT


The authors declare no conflict of interest.

DATA AVAILABILITY STATEMENT

Data involving simulations and optimizations can be made freely available on request by the readers.

ORCID

Fabio Corti  <https://orcid.org/0000-0001-8888-0388>

Gabriele Maria Lozito  <https://orcid.org/0000-0001-7987-0487>

REFERENCES

- El-Shahat, A., et al.: Electric vehicles wireless power transfer state-of-the-art. *Energy Procedia* 162, 24–37 (2019)
- Lee, C.H., et al.: Wireless power transfer system for an autonomous electric vehicle. In: 2020 IEEE Wireless Power Transfer Conference (WPTC), pp. 467–470. IEEE, Piscataway (2020)
- Li, S., Mi, C.C.: Wireless power transfer for electric vehicle applications. *IEEE J. Emerg. Sel. Top. Power Electron* 3(1), 4–17 (2014)
- Machura, P., De Santis, V., Li, Q.: Driving range of electric vehicles charged by wireless power transfer. *IEEE Trans. Veh. Technol.* 69(6), 5968–5982 (2020)
- Corti, F., et al.: A low-cost secondary-side controlled electric vehicle wireless charging system using a full-active rectifier. In: 2018 International Conference of Electrical and Electronic Technologies for Automotive, pp. 1–6. IEEE, Piscataway (2018)
- Mahesh, A., Chokkalingam, B., Mihet-Popa, L.: Inductive wireless power transfer charging for electric vehicles—A review. *IEEE Access* 9, 137667–137713 (2021)
- Triviño, A., González-González, J.M., Aguado, J.A.: Wireless power transfer technologies applied to electric vehicles: A review. *Energies* 14(6), 1547 (2021)
- Triviño-Cabrera, A., González González, J.M., Aguado, J.A.: *Wireless Power Transfer for Electric Vehicles: Foundations and Design Approach*. Springer, Cham (2020)
- Cirimele, V., et al.: Inductive power transfer for automotive applications: State-of-the-art and future trends. *IEEE Trans. Ind. Appl.* 54(5), 4069–4079 (2018)
- Hirata, A., et al.: Assessment of human exposure to electromagnetic fields: Review and future directions. *IEEE Trans. Electromagn. Compat.* 63(5), 1619–1630 (2021)
- Deruelle, F.: The different sources of electromagnetic fields: Dangers are not limited to physical health. *Electromagn. Biol. Med.* 39(2), 166–175 (2020)
- International Commission on Non-Ionizing Radiation Protection, et al.: Guidelines for limiting exposure to electromagnetic fields (100 kHz to 300 GHz). *Health Phys.* 118(5), 483–524 (2020)
- Cirimele, V., et al.: Human exposure assessment in dynamic inductive power transfer for automotive applications. *IEEE Trans. Magn.* 53(6), 1–4 (2017)
- Luca, P., et al.: Inductive power transfer: Through a bondgraph analogy, an innovative modal approach. In: 2017 IEEE International Conference on Environment and Electrical Engineering, pp. 1–6. IEEE, Piscataway (2017)
- Luca, P., Fabio, C., Alberto, R.: Application of wireless power transfer to railway parking functionality: Preliminary design considerations with series-series and lcc topologies. *J. Adv. Transp.* 2018, 1–14 (2018)
- Songcen, W., et al.: Electromagnetic shielding design for magnetic coupler of n-type dynamic electric vehicle wireless power transfer systems. In: 2019 22nd International Conference on Electrical Machines and Systems (ICEMS), pp. 1–7. IEEE, Piscataway (2019)
- Asa, E., et al.: Review of safety and exposure limits of electromagnetic fields (emf) in wireless electric vehicle charging (wevc) applications. In: 2020 IEEE Transportation Electrification Conference & Expo (ITEC), pp. 17–24. IEEE, Piscataway (2020)
- Canova, A., Giaccone, L.: A novel technology for magnetic-field mitigation: High magnetic coupling passive loop. *IEEE Trans. Power Deliv.* 26(3), 1625–1633 (2011)
- Stankiewicz, J.M.: Evaluation of the influence of the load resistance on power and efficiency in the square and circular periodic wpt systems. *Energies* 16(7), 2950 (2023)
- Stankiewicz, A., Stankiewicz, J.M., Choroszucho, A.: Numerical and circuit modeling of the low-power periodic wpt systems. *Energies* 13(10), 2651 (2020)
- Brizi, D., et al.: An accurate equivalent circuit model of metasurface-based wireless power transfer systems. *IEEE Open J. Antennas Propag.* 1, 549–559 (2020)
- Aditya, K., Williamson, S.S.: A review of optimal conditions for achieving maximum power output and maximum efficiency for a series-Series resonant inductive link. *IEEE Trans. Transp. Electrification* 3(2), 303–311 (2016)
- Kuperman, A.: Compensation capacitors sizing for achieving arbitrary load-independent voltage gain in series-series inductive wpt link operating at fixed frequency. *IEEE Trans. Power Deliv.* 35(6), 2737–2739 (2020)
- Nam, I., Dougal, R., Santi, E.: General optimal design method for series-series resonant tank in loosely-coupled wireless power transfer applications. In: 2014 IEEE Applied Power Electronics Conference and Exposition-APEC 2014, pp. 857–866. IEEE, Piscataway (2014)
- Yusoff, Y., Ngadiman, M.S., Zain, A.M.: Overview of nsga-ii for optimizing machining process parameters. *Procedia Eng.* 15, 3978–3983 (2011)
- Yuan, Y., Xu, H., Wang, B.: An improved nsga-iii procedure for evolutionary many-objective optimization. In: Proceedings of the 2014 Annual Conference on Genetic and Evolutionary Computation, pp. 661–668. ACM, New York (2014)
- Cardelli, E., Della Torre, E., Faba, A.: A general vector hysteresis operator: Extension to the 3-d case. *IEEE Trans. Magn.* 46(12), 3990–4000 (2010)
- Cardelli, E., et al.: Implementation of the single hysteron model in a finite-element scheme. *IEEE Trans. Magn.* 53(11), 1–4 (2017)
- Leonard, P.J., et al.: Finite element modelling of magnetic hysteresis. *IEEE Trans. Magn.* 31(3), 1801–1804 (1995)
- Reimers, A., et al.: Implementation of the preisach dok magnetic hysteresis model in a commercial finite element package. *IEEE Trans. Magn.* 37(5), 3362–3365 (2001)
- Canova, A., Grusso, G., Quercio, M., et al.: Characterization of electromagnetic device by means of spice models. *Int. J. Emerg. Technol. Adv. Eng.* 11(9), 12–22 (2021)

How to cite this article: Canova, A., Corti, F., Laudani, A., Lozito, G.M., Quercio, M.: Innovative shielding technique for wireless power transfer systems. *IET Power Electron.* 17, 962–969 (2024). <https://doi.org/10.1049/pel2.12580>